JOURNAL OF MATERIALS SCIENCE 27 (1992) 2147–2153

Desensitization of sensitized 304 stainless steel by laser surface melting

O. V. AKGUN, O. T. INAL
Department of Materials and Metallurgical Engineering, New Mexico Institute of Mining and Technology, Socorro, NM 87801, USA

Laser surface melting was used to desensitize the surface layer of sensitized 304 stainless steel. The degree of sensitization was determined quantitatively for sensitized and sensitized then laser surface melted samples from the modified ASTM-262 practice E test to be 45% and 0%, respectively. Grain-boundary melting which occurs in the heat-affected zone is believed to contribute the desensitization in the solid. X-ray diffraction results did not show any phase transformation in the melted layer or in the heat-affected zone. The results of the tensile tests indicate that sensitized stainless steel regains its corrosion resistance properties and, in addition, its mechanical properties seem to be enhanced by the laser surface melting.

1. Introduction

Although type 304 stainless steel is known for its high corrosion resistance, under some conditions such as improper thermal treatment, a sensitization problem renders this type of stainless steel susceptible to intergranular corrosion attack. Sensitization occurs by chromium carbide ($Cr_{23}C_6$) precipitation at grain boundaries during the slow cooling in the 450–900 °C temperature range. This chromium-rich carbide precipitation leads to the formation of a chromium-depleted zone adjacent to the grain boundaries. If the chromium content decreases to below 12% in the chromium-depleted zone, which is the minimum chromium limit for corrosion resistance, this zone becomes anodic to the rest of the grain with a big cathode/anode ratio that accelerates the corrosion process. To avoid the sensitization problem in type 304 stainless steel, the following steps are usually undertaken:

(i) a sufficiently high cooling rate is applied throughout the sensitization temperature range;

(ii) carbon stabilizing elements (e.g. titanium, niobium), that have a higher affinity to carbon than chromium, are added;

(iii) a low carbon-content stainless steel (e.g. type 304 L) is generally used.

An alternative approach to the avoidance of the sensitization problem in type 304 stainless steel can be laser treatment. Lasers are widely used in many applications that include surface modification of metals and alloys. Examples of laser surface treatments are surface hardening, surface melting and surface alloying. The heating of a metallic surface by the laser and the subsequent rapid cooling induces transformation hardening by martensite formation at the surface of some ferrous alloys [1–4]. This technique also finds application in the restoring of corrosion resistance on the surface of sensitized type 304 stainless steel [5]. Laser surface melting is another means of improving surface properties of metals and alloys. High cooling rates from the liquid state produce fine grains/dendrites which increase surface hardness and improve wear and corrosion resistance of alloys [6–16]. Anthony and Cline [15] reported the improvement of intergranular corrosion resistance of sensitized type 304 stainless steel through laser surface melting. They followed ASTM-262 practice E test for intergranular corrosion studies and also performed intergranular stress corrosion cracking tests for normalized, sensitized, and sensitized and laser surface melted stainless steels. Damborena *et al.* [16] studied the electrochemical behaviour of a sensitized and laser surface melted type 304 stainless steel and concluded that laser surface melting had a beneficial effect on the improvement of intergranular corrosion resistance of sensitized stainless steel.

The purpose of this study was to utilize the laser surface melting technique to study the desensitization of a sensitized type 304 stainless steel and determine quantitatively the effect of laser surface melting on the degree of sensitization.

2. Experimental methods

2.1. Materials

The composition of type 304 stainless steel used in this study is 0.058% C, 18.19% Cr, 9.14% Ni, 1.67% Mn, 0.36% Si, 0.020% S, 0.025% P, 0.32% Mo, 0.21% Cu and 0.066% N (by weight).

Two types of test specimens were used. Specimens that were subjected to ASTM-262 practice E solution had a diameter of 0.505 in (~ 1.28 cm) and 5 in (~ 12.7 cm) length. Those used in tensile testing had ASTM-A36 designation.

2.2. Laser surface melting

A GTE Sylvania Model 975 continuous-wave CO_2 laser, which provides a nominal output of 5000 W,

0022–2461

was used in these efforts. Specimens were scanned with 0.5 mm diameter beam at a speed of 7 mm s^{-1} and protected during the processing by a flowing argon gas shield. The laser processing apparatus is shown in Fig. 1.

For the ASTM-262 practice E test, specimens were surface melted by rotating and translating under the laser beam. This gave a melt depth of 1.2 mm. Melt paths for tensile test specimens were made parallel to the specimen surface to avoid any notch effect due to the melt path. A melt width of 1.8 mm and a depth of 1.2 mm were obtained. To ensure 50% overlapping for the melt paths, the specimen was rotated 7.2° about its major axis (Fig. 2). As a result, the melted zone covered almost 34% of the cross-sectional area of the specimen.

2.3. Intergranular corrosion test

To detect susceptibility to intergranular attack, ASTM-262 standard (practices A and E) test procedures were followed. Specimens were sensitized at 650 °C for 24 h to obtain chromium carbide precipitation at the grain boundaries and then water quenched. Following sensitization treatment, specimens were tested in an ASTM-262 practice A solution to screen the specimens before testing in practice E solution. After etching in 10 wt % oxalic acid solution, specimens were examined with an optical microscope at × 400. Ditch structure was observed along the grain and twin boundaries which were taken as an indication of sensitized structure.

For ASTM-262 practice E test, specimens were immersed in boiling copper–copper sulphate–16% sulphuric acid solution for 48 h. Bending tests were performed for sensitized, and sensitized and laser surface melted samples and checked for cracks on bent surfaces. No cracks were observed for sensitized and laser surface melted samples. However, deep cracks formed in the case of sensitized samples.

2.4. Tensile testing

ASTM-262 practice E is a qualitative test, thus, it is impossible to determine the contribution of laser surface melting to the desensitization of sensitized type 304 stainless steel from this test. Therefore, a modification of ASTM-262 practice E, with bend testing being replaced by tensile testing, was used as suggested by Muraleedharan *et al.* [17]. The degree of sensitization (DOS) was then determined from ultimate tensile strength (σ_{UTS}) by

$$DOS = \left(1 - \frac{\sigma_{UTS,\ exposed}}{\sigma_{UTS,\ unexposed}}\right) \times 100 \qquad (1)$$

Five types of specimens were tested at ambient temperature: as-received, as-received and laser surface melted, sensitized but not exposed to ASTM-262 practice E solution, together with sensitized and sensitized then laser surface melted samples that were exposed to ASTM-262 practice E solution. An MTS-810 model machine was used for the tensile testing.

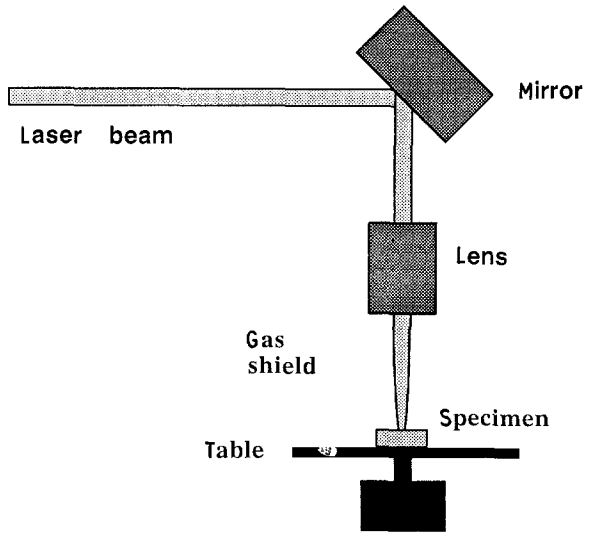

Figure 1 Laser processing apparatus.

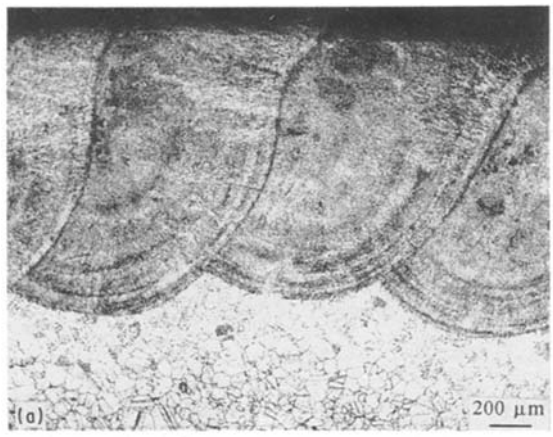

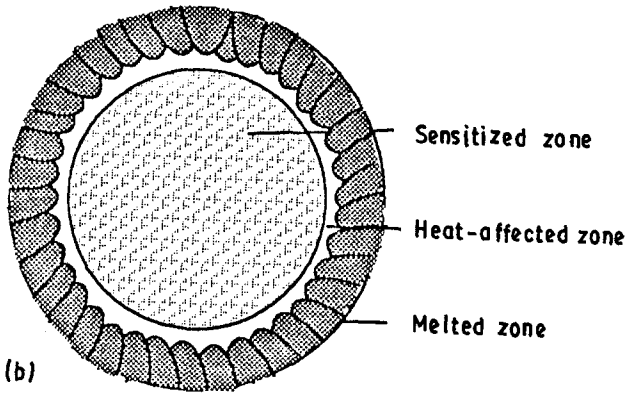

Figure 2 (a, b) Cross-section of a sensitized then laser surface melted 304 SS tensile test specimen (etched by 10% oxalic acid).

3. Results

Type 304 stainless steel is not amenable to martensitic transformation during rapid quenching to ambient, therefore, laser surface melting only causes microstructural changes such as a reduction in grain size as observed in the present experiments. Because the solidification mode for type 304 stainless steel is primary δ-ferrite [18, 19], this phase is seen to be present at the core of dendrites (Fig. 3).

The ASTM-262 practice A test reveals three types of distinct regions in sensitized and laser surface melted specimens (Fig. 4). The first one, which is in the laser melted region, does not show any chromium carbide

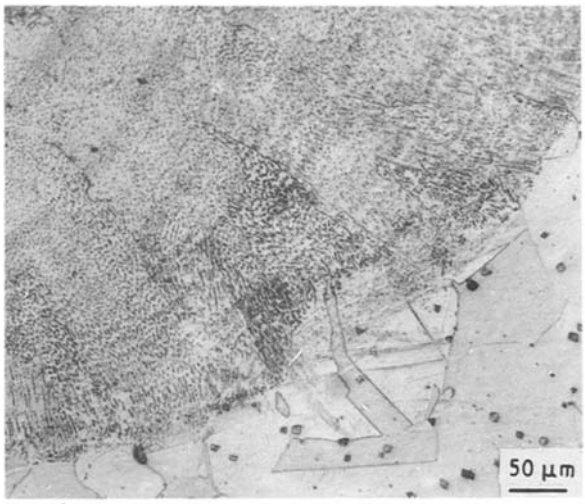

Figure 3 Epitaxial regrowth from the substrate in laser surface melted 304 SS.

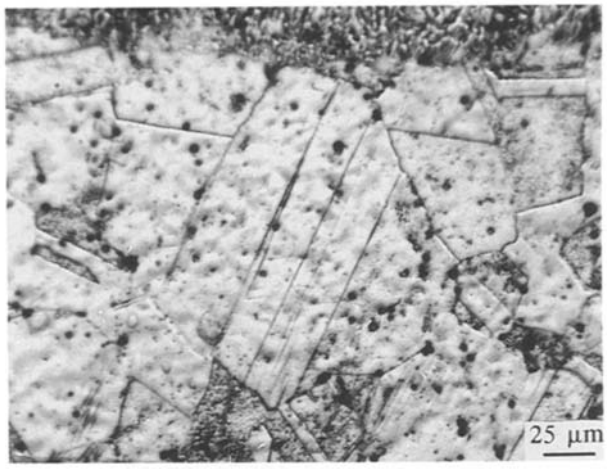

Figure 5 Disappearance of carbide precipitation in the heat-affected zone of sensitized then laser surface melted 304 SS after etching with 10% oxalic acid.

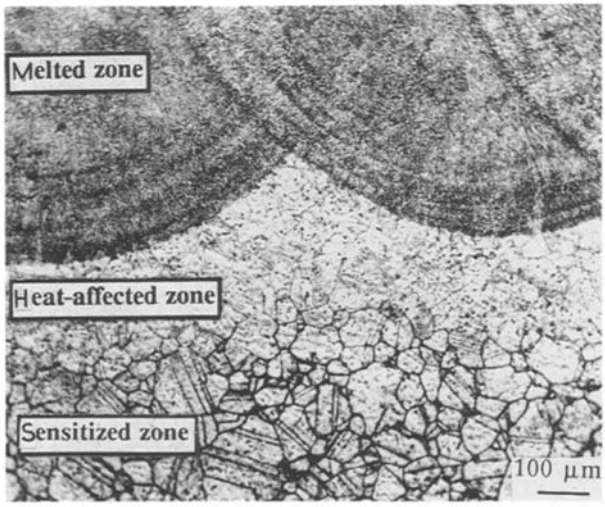

Figure 4 Microstructure of sensitized then laser surface melted 304 SS tensile test specimen after etching with 10% oxalic acid.

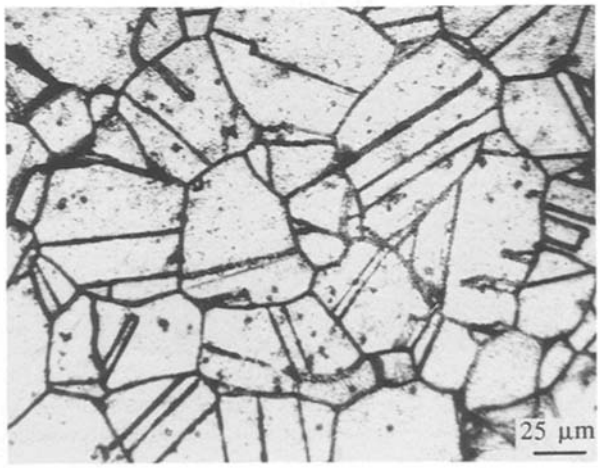

Figure 6 Carbide precipitation at the grain and twin boundaries in the sensitized region of 304 SS after etching with 10% oxalic acid.

TABLE I Tensile test results of the samples

	σ_{ys} (MPa)	σ_{uts} (MPa)
304 SS	324	620
304 SS + LSM	377	633
Sensitized[a]	186	322
Sensitized[b]	282	585
SEN + LSM	354	633

[a] Exposed.
[b] Unexposed.

precipitation. In the heat-affected zone (HAZ), the second region, precipitates of chromium carbide at grain and twin boundaries are seen to disappear following laser melting (Fig. 5). The HAZ has a thickness of 150 μm which covers almost 4% of the cross-sectional area of the tensile test specimen. The third region is the fully sensitized one and has a heavy chromium carbide precipitation along the grain and twin boundaries (Fig. 6).

Table I summarizes tensile test results for the specimens. Two different DOS values were determined from the tensile test made for ultimate strength evaluations. The first DOS value was obtained only from sensitized samples after exposure to the boiling Cu–$CuSO_4$–16% H_2SO_4 solution (Type I). However, the DOS values for sensitized and laser surface melted samples were calculated without exposure to the test solution because the surface layer was already desensitized (Type II). Typical DOS values for types I and II are 45% and 0%, respectively. Figs 7 and 8 show the fracture surfaces of sensitized and laser surface melted, and as-received and laser surface melted samples. It is interesting to see from Table I that both samples have almost the same yield and ultimate tensile strengths.

4. Discussion

4.1. Desensitization in the melted layer and the HAZ

Chromium carbides ($Cr_{23}C_6$) formed during the sensitization treatment are not stable at above 1000 °C. Because during laser surface melting (LSM), over a very short time, a thin surface layer reaches a very high

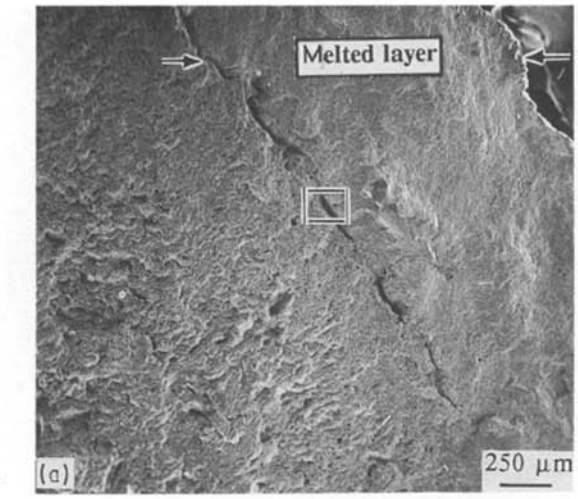

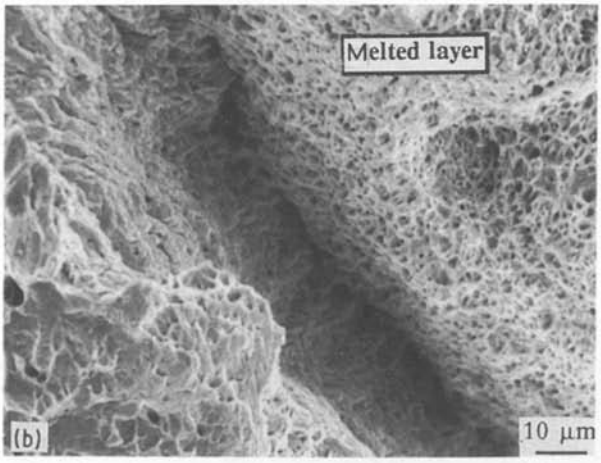

Figure 7 Scanning electron micrographs of fracture surfaces of (a) sensitized and laser surface melted 304 SS, and (b) higher magnification view of the area in the box in (a).

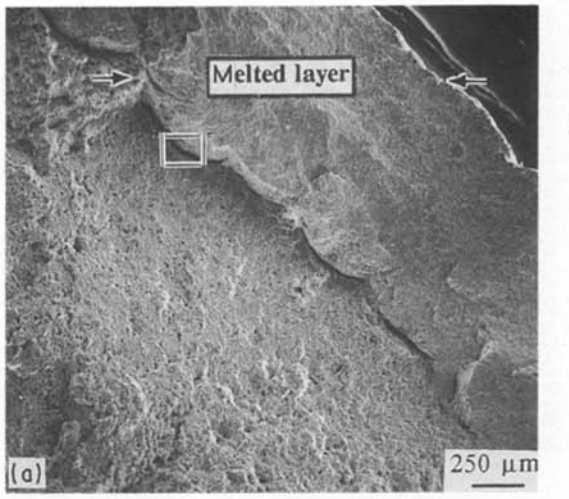

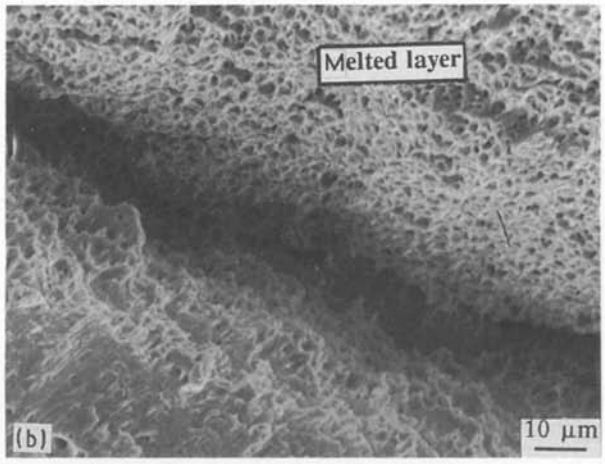

Figure 8 Scanning electron micrographs of fracture surface of (a) as-received and laser surface melted 304 SS, and (b) higher magnification view of the area in the box in (a).

temperature ($T_M \leqslant T \leqslant T_V$; where T_M and T_V are the melting and vaporization temperatures, respectively), all carbides are expected to decompose in the melted pool. Further redistribution of chromium in the melted pool is aided by two processes: diffusion in the liquid state and fluid flow/convection. The diffusion referred to here is due to the concentration difference of chromium in the chromium-rich carbide and the matrix.

The typical diffusion distance, X, in this process is a function of the diffusion constant in the liquid, D_L ($\sim 10^{-5}$ cm^2 s^{-1}) and time, t. If we assume that t, the duration of the melted pool, is simply related to the width of melted region and scan speed through

$$t = \frac{W}{V} \tag{2}$$

where W is the diameter of melted region, and V is scan speed, t is usually on the order of 10^{-1}–10^{-3} s. Then, the value for X varies between 10^{-3} and 10^{-4} cm. Also, the carbide thickness, after 24 h sensitization at 650 °C, is about 100 nm [20]. Because the diffusion distance, X, is larger than the carbide thickness, homogenization should occur through the diffusion process.

Studies on laser welding and surface alloying have shown that convection, which is induced by the temperature gradient at the free surface of the melted pool, controls the solute distribution [21–25]. It has been found that recirculating the velocity of the melted pool could be one or two orders of magnitude greater than the scanning velocity of the laser beam [23]. If this hypothesis is applied to our experimental conditions, it is clear that, when recirculating velocities reach values up to two orders of magnitude greater than the laser scan velocity, convection becomes a dominant process for chromium redistribution. It should also be emphasized that high power densities cause keyhole formation which, in turn, changes temperature gradients in the melted pool and thus an increase in fluid flow velocities [6].

During laser surface melting, the region outside the fusion zone will experience temperatures in the range of $T_M \leqslant T \leqslant T_{RM}$ (where T_{RM} is room temperature). Temperatures are high in the vicinity of the fusion line and decrease far from it. The nature of these temperature profiles depends on the interaction time and cooling rate. Isotherms which are favourable for carbide dissolution and chromium diffusion will form a desensitized region and these can be observed after

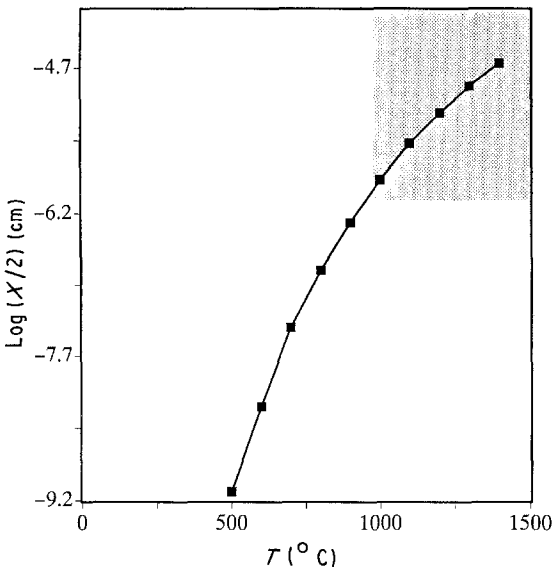

Figure 9 The relationship between the diffusion distance of chromium and temperature for an interaction time of 0.3 s. The shaded area represents the desensitized region obtained from the theoretical thickness of the chromium-depleted zone.

etching the samples with 10% oxalic acid solution (Fig. 4).

Fig. 9 shows the diffusion distances of chromium as a function of temperature in the γ-phase [26]. In this figure, the calculated value of chromium-depleted zone, about 10^{-6} cm [27], is compared with diffusion distances. It seems that chromium diffusion, for an interaction time of 0.3 s, can raise the chromium concentration in the chromium-depleted zone to that of the matrix. The corresponding temperature for this diffusion distance is around 975 °C, very close to the carbide dissolution temperature. Therefore, chromium diffusion is possible from the grains and the grain boundaries towards the chromium-depleted zone.

In our laser surface alloying study of 304 L with copper, we found copper to be present at the grain boundaries in HAZ, about 200 μm removed from the fusion line [28]. This was assumed to suggest that grain-boundary melting occurs in the HAZ. The reason why copper thus reveals the presence of melt in the grain boundaries is that copper has a low solubility in γ-phase and a low melting temperature with

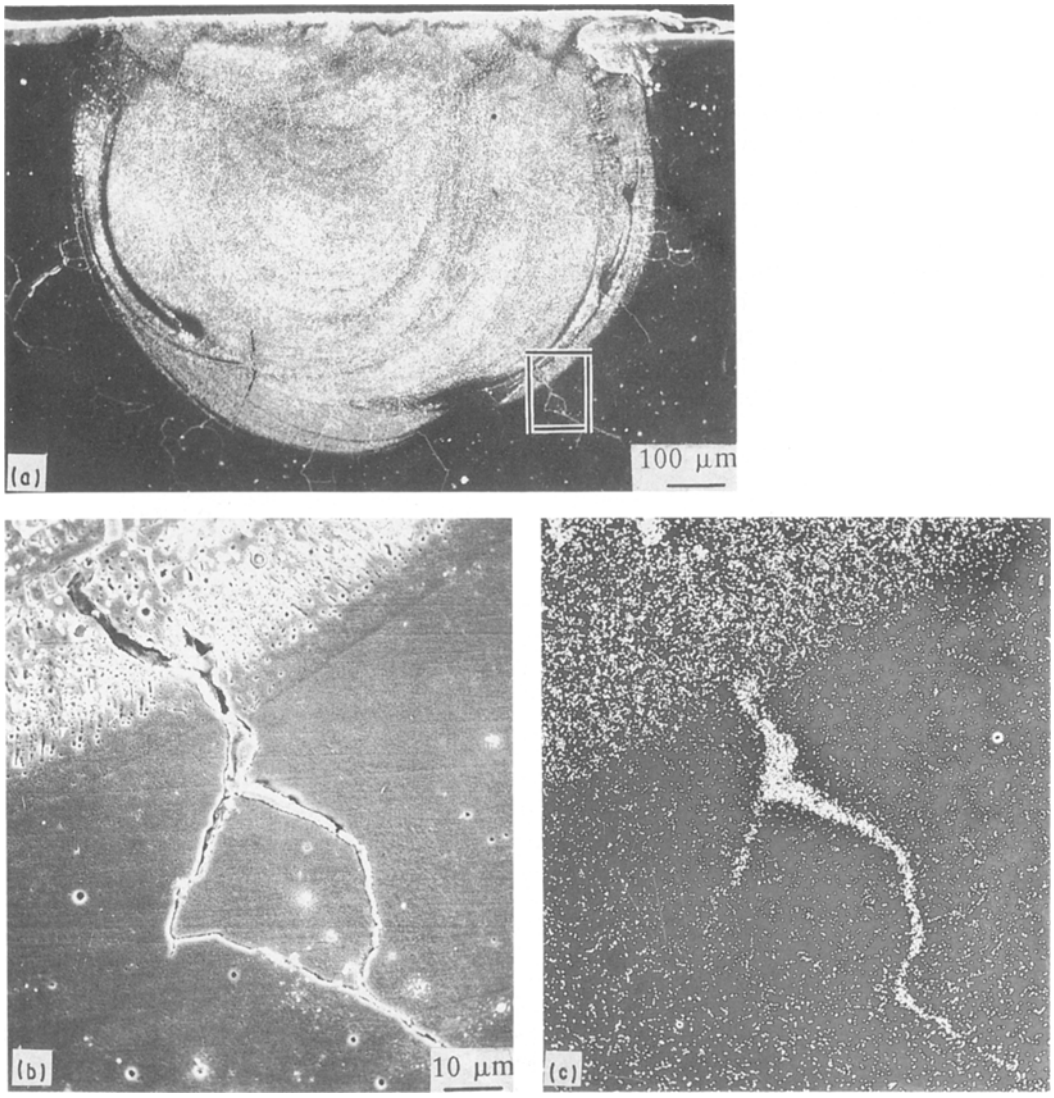

Figure 10 (a) Scanning electron micrograph of a laser surface melted copper-alloyed 304 L SS showing melted grain boundaries in the HAZ (laser power 5 kW, scanning speed 4.3 mm s^{-1}). (b) Higher magnification view of the area in the box in (a). (c) X-ray copper mapping of (b

respect to the 304 L substrate. Therefore, during laser surface melting, liquid copper must have penetrated into the melted grain boundaries and solidified there (Fig. 10). In light of this, one can assume that desensitization in the HAZ of the sensitized then laser surface melted samples is due to both solid state diffusion of chromium and grain-boundary melting taking place.

4.2. Tensile test results

There was no phase transformation observed in the melted layer or in the heat-affected zone. X-ray diffraction (XRD) data shows an increase in δ-ferrite content as well as the (1 1 1) peak intensity of the γ-phase in the melted layer (Fig. 11). Also, hardness data taken from the laser-melted layer shows about 30% increase in hardness. However, previous work has claimed martensite formation in the melted layer to have occurred because of the high cooling rate from the laser-melting temperature [15]. It should be kept in mind that the cooling rate is not a constant parameter in this case and decreases continuously during laser surface melting [29]. Furthermore, stress relief should occur in the melted zone when it becomes the HAZ for the next melt path. Therefore, the assumption of martensitic transformation based on a high cooling rate should not be valid.

The degree of sensitization value of type II samples indicates that laser surface melting shows an increase in the mechanical properties of sensitized type 304 stainless steel. Yield and ultimate tensile strengths of sensitized and laser surface melted samples exceed those of the as-received material (Table I). This increase emanates from the microstructure of the melted layer. Because laser melting produces very small grains/dendrites, and they grow perpendicular to the sample surface, this causes textured structure in the melted layer which, in turn, exhibits the enhanced properties.

The yield strength of the laser-melted layer was calculated to be about 485 MPa which is 50% higher than for the as-received ones. If the Hall–Petch relation is considered, this amount of increase in yield strength is consistent with decreasing grain size in the laser melted layer. In addition to that, the extent of the textured structure of the laser-melted layer, even though it is hard to determine, should contribute to an increase in yield strength. However, Anthony and Cline [15] reported a ten-fold increase in yield strength of the laser-melted layer obtained through a slow strain rate test performed at 289 °C. They attributed this high yield strength value to the previously mentioned formation of martensite in the laser-melted layer. In the present investigation, the XRD data (Fig. 11) as well as hardness values obtained from the laser-melted layer support the absence of martensitic transformation in the laser melted layer. Therefore, an increase in yield strength is not due to martensitic transformation. It seems that any explanation given to this increase at 289 °C should consider the temperature dependence of the yield strength of the laser-melted layer.

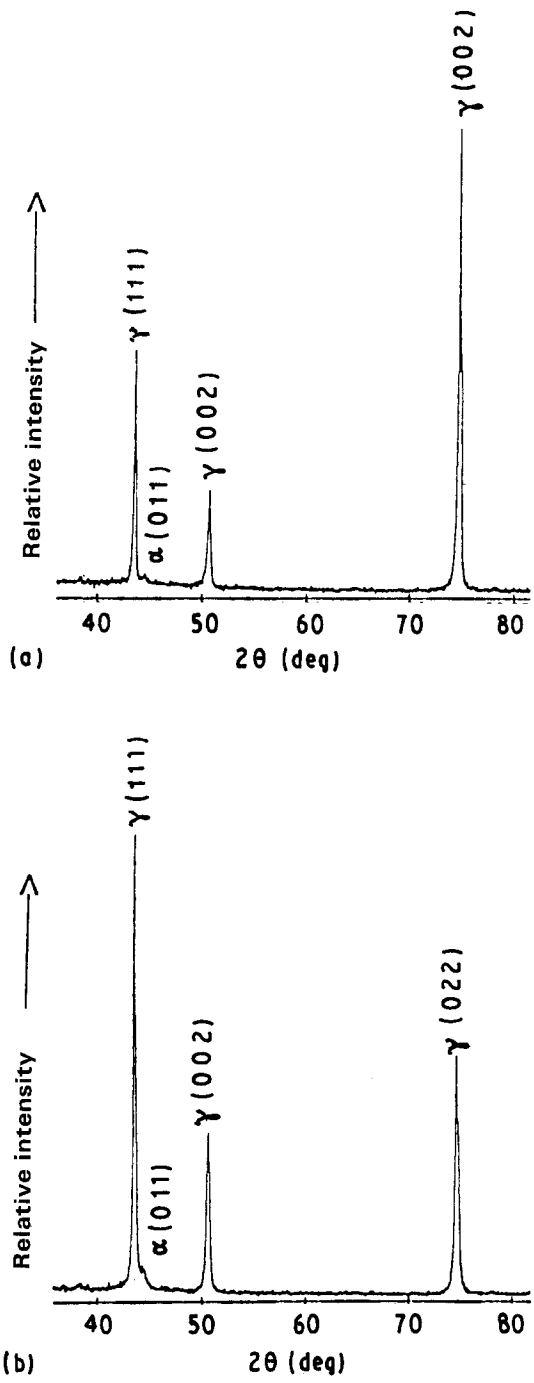

Figure 11 XRD patterns taken from the surface of (a) as-received, (b) as-received then laser surface melted 304 SS.

The fracture surfaces of both sensitized and laser surface melted, and as-received and laser surface melted samples are shown in Figs 7 and 8. The change in appearance of the fracture surfaces clearly indicates a change in microstructure in the laser-melted and unmelted regions for both cases. Also, the reduction in cross-sectional area for both samples was found to be small in comparison to the as-received and the sensitized samples. One similarity in the appearance of the fracture surfaces is the presence of boundary separation between the melted and unmelted regions. It is possible that incompatability in plastic deformation causes this boundary separation and leads to material failure. However, further study is needed to elucidate the fracture behaviour of this composite structure.

5. Conclusions

1. Laser surface melting improves the intergranular corrosion resistance as well as mechanical properties of sensitized type 304 stainless steel.

2. The contribution of laser surface melting to the degree of sensitization was determined quantitatively from the modified ASTM-262 practice E test.

3. Grain-boundary melting occurs in the HAZ of sensitized then laser melted type 304 stainless steel and causes the desensitization in this area as well.

4. There is no phase transformation observed in the laser-melted layer of type 304 stainless steel.

5. The yield strength of the laser-melted layer is about 50% higher than that of the as-received type 304 stainless steel.

References

1. S. KOU, D. K. SUN and Y. P. LE, *Metall. Trans.* **14A** (1983) 643.
2. S. MANDZIEJ, M. C. SEEGERS and J. GODJIK, *Mater. Sci. Tech.* **5** (1989) 350.
3. J. R. BRADLEY and S. KIM, *Script. Metall.* **23** (1989) 136.
4. Y. W. KIM, P. R. STRUTT and H. NOWOTNY, *Metall. Trans.* **10A** (1979) 881.
5. Y. NAKAO and K. NISHIMOTO, *Trans. Jpn. Weld. Soc.* **17** (1986) 84.
6. P. R. STRUTT, *Mater. Sci. Engng* **44** (1980) 239.
7. B. H. KEAR, E. M. BREINAN and L. E. GREEWALD, *Met. Technol.* **6** (1979) 121.
8. G. CHRISTODOULOU, A. WALKER, W. M. STEEN and D. R. F. WEST, *ibid.* **10** (1983) 215.
9. J. KUSINSKI, *Metall. Trans.* **19A** (1988) 377.
10. H. de BEURS, J. A. HOVIUS and J. Th. M. de HOSSON, *Acta Metall.* **36** (1988) 3123.
11. H. W. BERGMAN, in "Laser Surface Treatment of Metals", edited by C. W. Draper and P. Mazzoldi (NATO ASI Series, Martinus Nijhoff, Dordrecht, Netherlands, 1986) p. 351.
12. T. R. JERVIS, D. R. BAER and D. J. FRYDRYCH, *Mater. Lett.* **6** (1988) 225.
13. D. S. GNANAMUTHU, in "Applications of Lasers In Materials Processing", edited by E. A. Metzbower, *et al.* (ASM, Metals Park, 1979) p. 239.
14. E. Mc CAFFERTY and P. G. MOORE, *J. Electrochem. Soc.* **133** (1986) 1090.
15. T. R. ANTHONY and H. E. CLINE, *J. Appl. Phys.* **49** (1978) 1248.
16. J. de DAMBORENA, A. J. VAZQUEZ, J. A. GONZALEZ and D. R. F. WEST, *Surf. Engng* **5** (1989) 235.
17. P. MURALEEDHARAN, J. B. GNANAMOORTHY and K. PRASAD RAO, *Corrosion* **45** (1989) 149.
18. J. C. LIPPOLD and W. F. SAVAGE, *Weld. J.* **59** (1979) 362s.
19. *Idem., ibid.* **59** (1980) 48s.
20. C. S. TEDMON Jr, D. A. VERMILYA and J. H. ROSOLOWSKI, *J. Electrochem. Soc.* **118** (1971) 192.
21. T. CHANDE and J. MAZUMDER, "Lasers in Metallurgy", edited by K. Mukherji and J. Mazumder (The Metallurgical Society of AIME, Warrendale, PA, 1981) p. 165.
22. T. CHANDE and J. MAZUMDER, *Appl. Phys. Lett.* **41** (1982) 42.
23. C. CHAN, J. MAZUMDER and M. M. CHEN, *Metall. Trans.* **15A** (1984) 2175.
24. T. CHANDE and J. MAZUMDER, *J. Appl. Phys.* **57** (1985) 2226.
25. A. PAUL and T. DEBROY, *Metall. Trans.* **19B** (1988) 851.
26. C. STAWSTRÖM and M. HILLERT, *J. Iron. Steel. Inst.* **207** (1969) 77.
27. P. CHUNG and S. SZKLARSKA-SMIALOWSKA, *Corrosion* **37** (1981) 39.
28. O. V. AKGUN and O. T. INAL (1989) unpublished.
29. T. ZACHARIA, S. A. DAVID, J. M. VITEK and T. DEBROY, *Metall. Trans.* **20A** (1989) 957.

Received 7 January
and accepted 13 May 1991